Biosensors and Bioelectronics 96 (2017) 213–219

Contents lists available at ScienceDirect

Biosensors and Bioelectronics

journal homepage: www.elsevier.com/locate/bios

A Point-of-Need infrared mediated PCR platform with compatible lateral flow strip for HPV detection

Wenjia Liu[a], Mingfang Zhang[b], Xiaoyan Liu[a], Alok Sharma[a], Xianting Ding[a,*]

[a] State Key Laboratory of Oncogenes and Related Genes, Institute for Personalized Medicine, School of Biomedical Engineering, Shanghai Jiao Tong University, Shanghai 200030, China

[b] Gene Company Limited, Jingzhuang business center, No.772 Yingtian Street, Jianye District, Nanjing 210000, China

ARTICLE INFO

Keywords:
Infrared LED
PCR
Microfluidic
Point-of-Need testing
Lateral flow strip

ABSTRACT

With the increasing need of monitoring the epidemiology of serious infectious diseases, food hygiene, food additives and pesticide residues, it is urgent to develop portable, easy-to-use, inexpensive and rapid molecular diagnostic tools. Herein, we demonstrate a prototype of IR mediated Conducting Oil and CarbOn Nanotube circUlaTing PCR (IR-COCONUT PCR) platform for nucleic acid amplification. The presented platform offers a new solution for miniaturized PCR instruments with non-contact heaters by using conducting oil and carbon nanotube as a medium in IR mediated PCR. This novel platform offers accurate and flexible control of temperature through the integration of PID (proportional–integral–derivative) algorithms to manipulate the duty cycle of the voltage signals of IR LED and a peristaltic pump. The ramping rate of the introduced platform in current study is 1.5 °C/s for heating speed and −2.0 °C/s for cooling speed. This platform fulfills 30 thermal cycles within 50 min which is a match to the conventional bench-top PCR thermo cyclers. For demonstration purpose, human papillomavirus (HPV) patient cervical swab specimens were examined. Downstream lateral flow strip (LFS) was also developed to quantity the PCR products from the IR-COCONUT PCR device within 25 min. This PCR platform together with the compatible LFS shows great potential for in-field and Point-of-Need (PoN) testing of genetic or contagious diseases.

1. Introduction

Point-of-Need (PoN) testing, a new concept which has been proposed to enrich Point-of-Care (PoC) testing, is defined as any diagnostic test that can be performed out of reference laboratories, such as home, patient's bed, ICUs, physician's office or production line, etc. (Benjamin and Sébastien, 2016). PoC testing relates to human testing whereas PoN testing refers to a much larger scope, including human testing (Chuang et al., 2016; Lee et al., 2015; Wang et al., 2012), veterinary testing (Tarasov et al., 2016), industrial testing (Wang et al., 2017), argo-food testing (Raeisossadati et al., 2016), environmental testing (Bidmanova et al., 2016; Gomes and Sales, 2015), forensics (Soejima and Koda, 2014) and so on. Since the first applications of PoC testing in 1990s, microfluidic technology has been used to solve technical problems and it has become part of the diagnostics revolution in the healthcare industry. The emerging field of microfluidic technology in combination with Micro-Electro-Mechanical Systems (MEMS) can provide exciting solutions to PoN testing. Bio-analytical systems based on microfluidics and MEMS can allow for miniaturization and integration of processes onto a chip with benefits including test speed, cost, portability and automation.

With the increasing need of monitoring the epidemiology of serious infectious diseases, food hygiene, food additives and pesticide residues, particularly in developing countries with poor infrastructure or on-site detection with the need of rapid results, it is urgent to develop portable, easy-to-use, inexpensive and rapid molecular diagnostic tools. In recent advances, lateral flow assays (LFAs) (Ahrberg et al., 2016; Choi et al., 2016; Raston et al., 2016; Rodriguez et al., 2016) have been used to achieve simple and cost-effective nucleic acid testing. LFAs are capable of producing semi-quantitative results by fluorescence signals or visible color formation in less than 30 min. However, the constituent of biological samples (e.g., blood, urine and saliva) are generally complex and contain low amounts of target nucleic acids. Prior to lateral flow detection, the sample pretreatment, off-chip extraction/solid-phase extraction and amplification processes (polymerase chain reaction (PCR)) are normally required.

Miniaturized PCR instruments (Ahrberg et al., 2016; Chung et al., 2010; Liu et al., 2004; Park et al., 2016) utilize both MEMS and microfluidic technology to fulfill the conventional PCR functions onto a

* Corresponding author.
E-mail address: dingxianting@sjtu.edu.cn (X. Ding).

http://dx.doi.org/10.1016/j.bios.2017.04.047
Received 25 January 2017; Received in revised form 26 April 2017; Accepted 27 April 2017
Available online 29 April 2017
0956-5663/ © 2017 Elsevier B.V. All rights reserved.

portable device that can be used in any condition and capable of rapid target gene identification. Many miniaturized PCR devices have exhibited superior performance than bench-top PCR thermo cyclers in the aspects of cost, ramping speed, portability, integration level, efficiency, etc. Based on the design of sample chambers, miniaturized PCR instruments can be categorized into static chamber PCR (Sposito et al., 2016; Zhu et al., 2014) and continuous flow PCR (Chung et al., 2010). The static chamber PCR resemble the bench-top PCR thermo cyclers as the sample is kept in a small chamber and undergoes a continuous temperature cycle. The sample in continuous flow PCR travels repeatedly through three temperature zones for amplification purpose. The design of static chamber PCR could be more impact than the continuous flow PCR and the number of cycles is easier to alter based on demands. However, the temperature ramping rate of static chamber PCR is lower than the continuous flow PCR. Over the years, various on-chip heaters have been demonstrated to improve the speed of temperature cycling. In general, the heaters have two categories, namely contact type (thin films, metal heating blocks and Peltier units) and non-contact type (IR, microwave and laser heater units). The ramping speed of micro-fabricated thin film can achieve 175 °C/s for heating speed and −125 °C/s for cooling speed and fulfill 40 thermal cycles within 6 min (Neuzil et al., 2006). But the contact heaters have the demerit of complexity and cost of fabrication. On the other hand, the compact heater design which reduces the thermal mass of the whole chip is essential to achieve fast temperature cycling speed. The non-contact heaters are more favorable for simple design and flexible system integration. As the heaters do not have to contact the sample chamber, it offers more opportunities to utilize multiple chip designs upon the same platform. Several researchers have successfully integrated IR-mediated (Hühmer and Landers, 2000; Hagan et al., 2011; Legendre et al., 2006) or laser assisted heater units (Slyadnev et al., 2001) to directly heat the PCR sample and achieved amplicon detection. The previous IR-mediated PCR utilizes a high-power tungsten lamp and convex lens to heat the sample directly. This method suffers a great heat loss due to the large thermo mass and has a limitation to conduct multi-chamber PCR at the same time.

In the present study, we developed a prototype of IR mediated Conducting Oil and CarbOn Nanotube circUlaTing PCR (IR-COCONUT PCR) platform for nucleic acid amplification. This platform can fulfill both thermal cycling like three stage/two stage PCR and isothermal amplification like Loop-Mediated Isothermal Amplification (LAMP), Strand Displacement Amplification (SDA), Helicase Dependent Amplification (HDA), etc. For demonstration purpose, human papillomavirus (HPV) was applied as a model analyte to examine the three-stage temperature cycle performance of this IR-COCONUT PCR. The PCR products were detected by lateral flow strip with less than 25 min.

2. Material and methods

2.1. Microfluidic chip design and fabrication

The structure of PCR microfluidic chip is illustrated in Fig. 1A. This chip was constructed using a five layer stack consisting of an upper cover layer, a PCR chamber layer, a copper layer, a conducting oil layer and a lower cover layer. All the four layers apart from the copper layer were made of PMMA with 1 mm thickness. In the PCR chamber layer, three identical oval shaped channels (20 μL) were fabricated (Fig. 1B) to expel dead zone air when introducing samples to the channels. The middle channel was filled with water and connected to a thermocouple to implement feed-back control of the three-stage temperature cycles during PCR. The other two channels were designed as the sample chambers. There were also four L-shape materials removed from the PCR chamber layer to reduce the thermal mass of the whole chip. In the conducting oil layer, a square shape spiral channel (700 μm in width), as illustrated in Fig. 1B, was lying right beneath the three PCR chambers. The spiral channel was connected to a peristaltic pump and an oil tank by polytetrafluoroethylene (PTFE) tubes. The oil in the oil tank was a mixture of conducting oil (Mobiltherm) and multi-walled

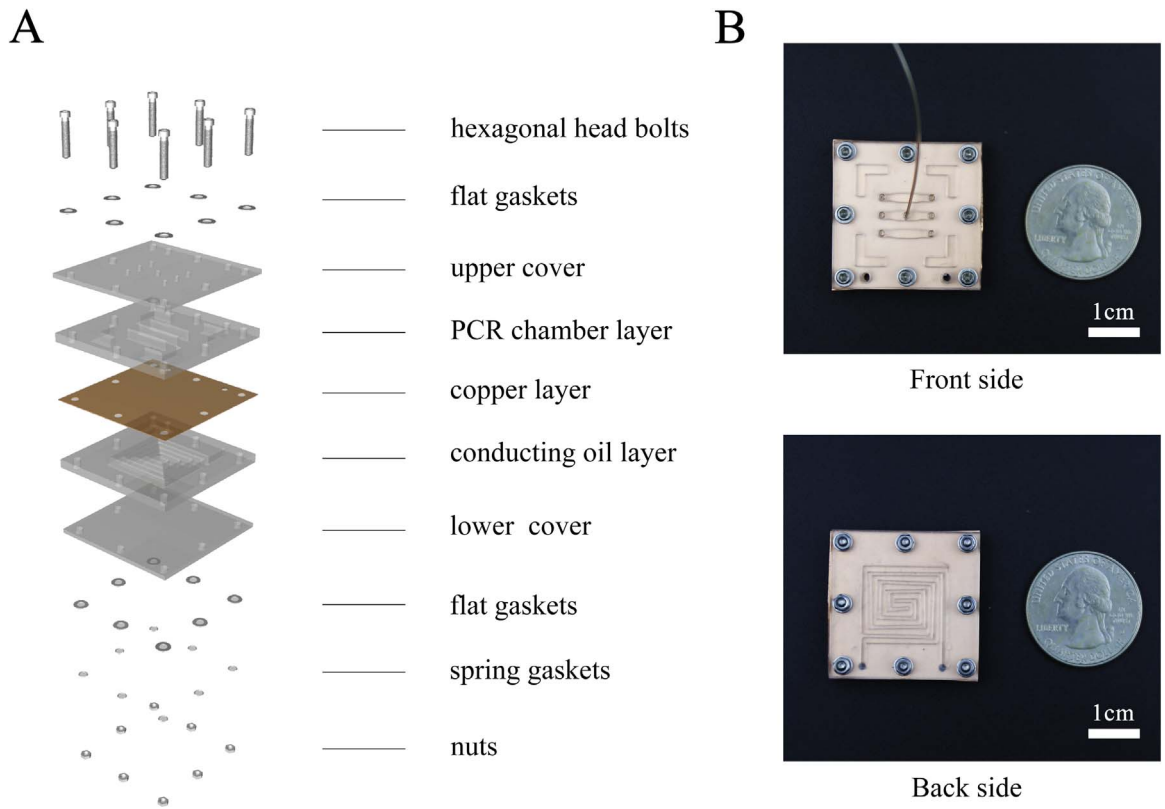

Fig. 1. The scheme of PCR microfluidic chip. (A) The assembly exploded diagram of PCR microfluidic chip. (B) The front side and back side of assembled PCR microfluidic chip.

carbon nanotube (MWNT) at a concentration of 4 mg/ml. The copper layer was made of copper sheet with 100 μm in thickness to transfer heat from the conducting oil to the PCR chambers and balance the temperature within the heated zones.

The fabrication process of the microfluidic chip was formed as follows: The patterns were first designed by Adobe Illustrator and sent to the laser engraving machine (Gravograph LS100, Gravotech Group, France). After the PMMA materials were laser ablated, the copper layer was cut by a cutting machine and drilled by a hand hold drilling machine to fabricate the holes for PTFE tubes and hexagonal head bolts. All the layers were rinsed by ethanol and DI water before assembling. After dried by nitrogen gas, the five layers of the PCR microfluidic chip were carefully fastened by hexagonal head bolts, flat gaskets, spring gaskets and nuts to prevent leakage. Then the thermocouple was inserted into the middle PCR chamber and sealed with silica gel. After the middle chamber was filled with water and the other two chambers were filled with samples, all the three chambers were sealed with ARseal™ adhesive tape (Adhesives Research, Inc., Glen Rock, PA) during operation.

2.2. IR-COCONUT PCR platform design

The IR-COCONUT PCR platform consisted of an infrared LED (20 W, 850 nm), a peristaltic pump (NKP-DC-B06B, Kamoer), an oil tank, a thermocouple (TT-K-36-SLE, ETA), a data acquisition card (USB-DAQ-XF103, Antech Enterprise Limited), a thermocouple cold junction compensation circuit, a LED circuit and a pump circuit (Fig. 2A). The principle of the PCR platform is illustrated in the three-dimension effect graph (Fig. 2B & C) rendering by Autodesk Maya. Both the voltage signals of the peristaltic pump and infrared LED were controlled by PID algorithms. By varying the duty cycle of the voltage signals, a pulse-width modulation (PWM) control technology was established. With longer duty ratio of the LED voltage signal, more power would generate to and heat the MWNT more quickly. Similarly, with longer duty ratio of the pump voltage signal, flow rate would increase and the heated oil would be expelled out of the microfluidic chip and replaced with unheated oil from the oil tank. Thus the maximum heating rate was realized by outputting the rated power of the LED and turning off the pump, while the maximum cooling rate was realized by outputting the rated power of the pump and turning off the LED. Two separate PID controllers, one for the LED and one for the pump, when optimized, were applied to modulate the temperature ramping rate and stabilize the temperature.

2.3. Sample pretreatment, PCR verification and gel electrophoresis

Patient cervical swab specimens were collected from the volunteers in International Peace Maternity & Child Health Hospital (Shanghai, China) and de-identified. The clear supernatant solution of the specimens was removed after centrifugation at 1500 rpm for 5 min. Then the bottom sediments were rinsed by PBS and the supernatant was also removed after centrifugation at 1500 rpm for 5 min 45 μL of NaOH (50 nM) was added to the sediments and heated to 95 °C for 1 h to extract the genome DNA. Finally, 5 μL of Tris-HCl (1 M, pH 8.0) was added to the sample. The DNA concentration of the samples was measured by NanoDrop 2000C (Thermo Fisher, USA).

Biotinylated forward primer: 5'- BIO/AAGGGCGTAACCGAAAT CGGT-3'.

Digoxigenin labeled reverse primer: 5'- DIG/GTTTGCAGCTCTGT GCATA-3'.

The primer sequences amplified a 140 bp fragment. The 20 μL PCR sample mixture was composed of 2 μL of 10×Ex Taq buffer (Takara, Japan) , 1.6 μL of dNTP mixture, 0.5 μL of each primer (10 μM), 1 μL of pretreated patient sample, 0.1 μL of Takara Ex Taq (Takara, Japan) and 14.3 μL of DI water. A conventional thermal cycler (LightCycler®96, Roche, Switzerland) was used as a standard conventional PCR control. The thermal cycling protocol was set as preheat at 94 °C for 5 min, followed by 30 cycles of 94 °C for 30 s, 55 °C for 30 s, 72 °C for 15 s, and a final extension step for 10 min at 72 °C. Then the PCR products were mixed with 2 μL buffer and were electrophoretically analyzed on a 2% agarose gel at 100 V for 30 min together with the 100 bp DNA ladder (TIANGEN, Beijing).

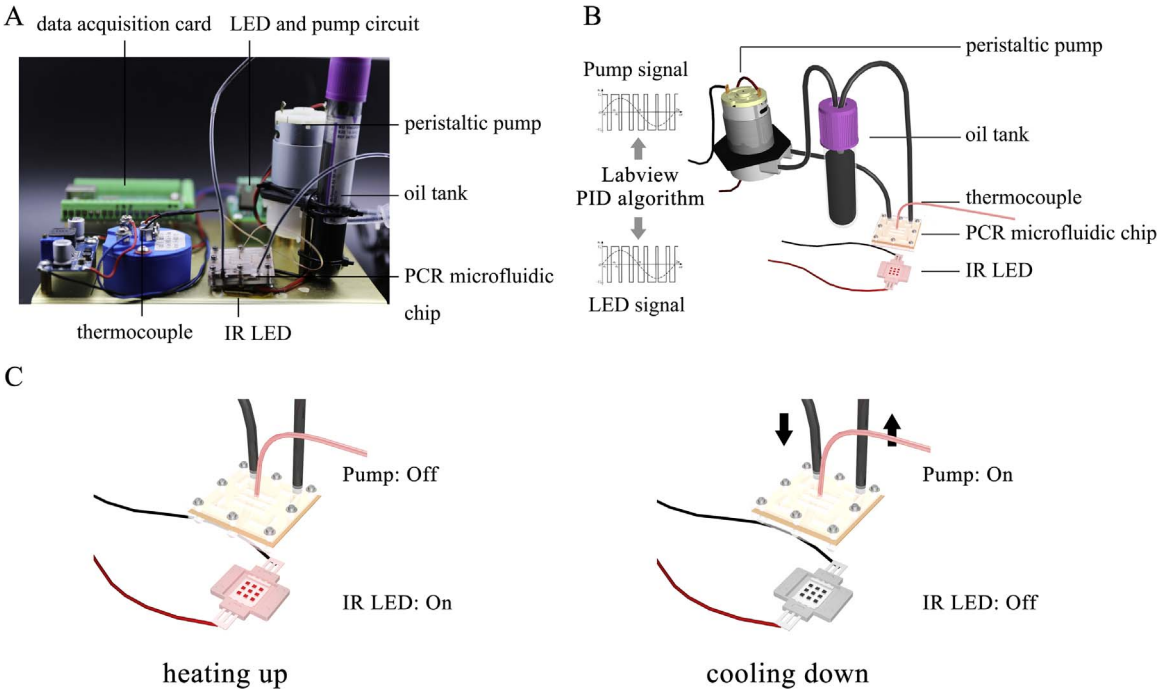

Fig. 2. The scheme of IR-COCONUT PCR platform. (A) The physical illustration of IR-COCONUT PCR. (B) The work principle of IR-COCONUT PCR platform. (C) The demonstration of temperature control for on-chip heating and cooling.

2.4. Preparation of the lateral flow strip (LFS)

The LFS consisted of sample pad (JY-Y107, Jieyi Biotechnology, Shanghai), conjugate pad (JY-BX101, Jieyi Biotechnology, Shanghai), nitrocellulose pad (NC-a110, Millipore), absorbent pad (JY-X115, Jieyi Biotechnology, Shanghai) and baseboard (JY-D103, Jieyi Biotechnology, Shanghai). The sample pad was soaked into the sample buffer which contained 0.05 M Tris–HCl, 0.15 mM NaCl (pH8.0), 0.25% TritonX-100% and 2.5% Tween-20. The goat-anti-rabbit IgG in antibody buffer (0.01 M TBS(pH7.4) with 1% BSA, 0.03% Proclin300 and 50% Glyce) was added to the conjugate pad. Then the sample pad and conjugate pad were dried at 37 °C overnight and stored in desiccators at room temperature. The test and control zones on the nitrocellulose pad were dispensed at an optimized concentration of streptavidin (test zone) and anti-digoxigenin- alkaline phosphatase(AP) conjugates (control zone) respectively. Then the nitrocellulose pad was dried at 37 °C for 2 h. Finally, nitrocellulose pad, absorbent pad, conjugate pad and sample pad were assembled sequentially onto the baseboard which contained an adhesive layer. Both the absorbent pad and conjugate pad should overlap 2 mm of the nitrocellulose to ensure the sample solution could migrate through the test strip during the PCR product detection assay.

2.5. PCR product detection assay procedure

The PCR products, DI water, anti-digoxigenin-AP conjugates and BCIP (5-Bromo-4-Chloro-3-Indolyl Phosphate) /NBT (Tetranitroblue tetrazolium chloride) stock solution (R21319, Yuanye Biotechnology Limited, Shanghai) were added sequentially to the test strip. The color reaction on the test and control zones could be visualized within 25 min. The digital images of the test strips can be either obtained by a cell phone or a digital camera. Then the images were transferred to the computer and converted to 32-bit formats by Image J software. The concentration of the PCR products was quantitatively analyzed by comparing the optical intensities of the test zone and the control zone by Imagine J (Qiu et al., 2015).

3. Results and discussion

3.1. Comparison between IR-COCONUT PCR and conventional bench-top PCR

The heating and cooling speed and accuracy of temperature is influenced by several parameters. Firstly, the LED light power, carbon nanotube concentration, maximum flow rate of the peristaltic pump need to be decided. For instance, the LED power should be high enough to heat up the conducting oil to more than 95 °C in a short time and it should be low enough to save electricity power. The most important optimization of the temperature is to find the proper PID parameters (proportional term, integral term and derivative term). Without proper tuning of these terms, the PID controller can be inaccurate and oscillating.

The ramping speed and gel electrophoresis results comparison between IR-COCONUT PCR and LightCycler®96 is illustrated in Fig. 3. The ramping speed of the IR-COCONUT PCR is a match to the conventional bench-top PCR thermo cyclers. As in Fig. 3B, both of the IR-COCONUT PCR and LightCycler®96 showed a bright target DNA band which indicated successful nucleic acid amplification. However, the DNA product of IR-COCONUT PCR did show slightly more dimers than the LightCycler®96. This observation could be attributed to the fact that the microfluidic chip of IR-COCONUT PCR was exposed to the open air and temperature fluctuation occurred during the operating process.

3.2. Optimization of IR-COCONUT PCR setups

To obtain the best performance of IR-COCONUT PCR, parameters including annealing temperature, extension time, denaturation and annealing time were optimized. Patients' samples were preheated at 94 °C for 5 min, followed by 30 cycles of 94 °C for 30 s, 55 °C for 30 s, 72 °C for 15 s, and a final extension step for 10 min at 72 °C (Fig. 4A). The sample in lane 14 was chosen to conduct the following optimization because it had the brightest target band and fewer smears. Then the annealing temperature was varied from 51 °C to 59 °C (Fig. 4B). The optimized annealing temperature was set to be 59 °C because it had fewer smears than other temperatures. The extension time was varied from 10 s to 20 s, and set as 10 s according to the results in Fig. 4C because the intensity of smears in 10 s was less than other conditions. Similarly, the optimized denaturation and annealing time was set as 20 s (Fig. 4D). Finally, the PCR product was verified for its monoclonal sequence and the 140 bp sequences of the HPV 16 gene were successfully obtained as shown in Fig. 4E.

3.3. Design of the LFS measurement

In order to facilitate the PoN application of the presented IR-COCONUT PCR, LFS compatible with the current setup was also developed. Fig. 5A illustrates the principle of the HPV 16 detection on the LFS. After the PCR products and DI water were applied to the sample pad, the solution migrated by capillary force. If the patient's cervical swab specimen was HPV 16 positive, the reaction between targeted DNA (degoxigenin end) and anti-digoxigenin-AP conjugates

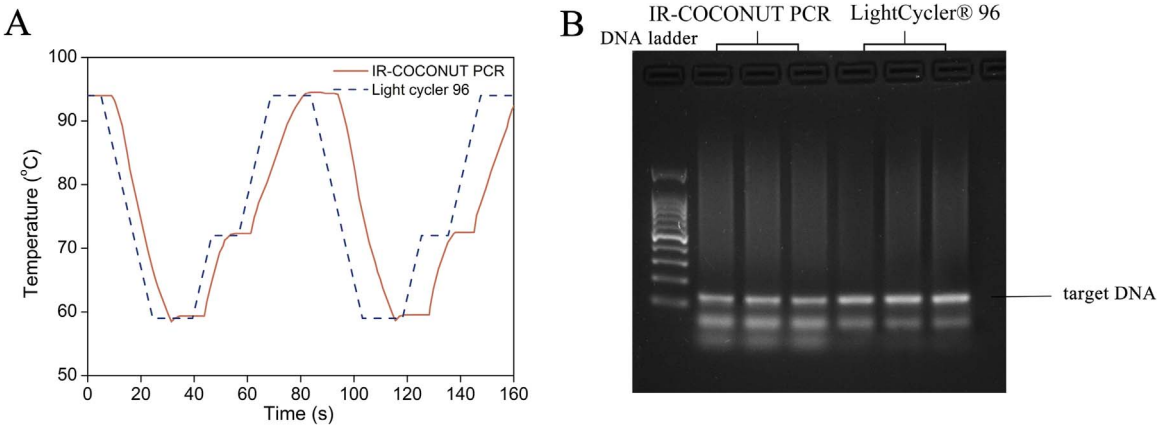

Fig. 3. The comparison between IR-COCONUT PCR and commercial LightCycler®96. (A) The temperature ramping speed comparison suggested the presented IR-COCONUT PCR is a peer to commercial equipment. (B) The gel electrophoresis comparison indicated both platforms could successfully amplify nucleic acid. Each sample was independently detected for 3 times.

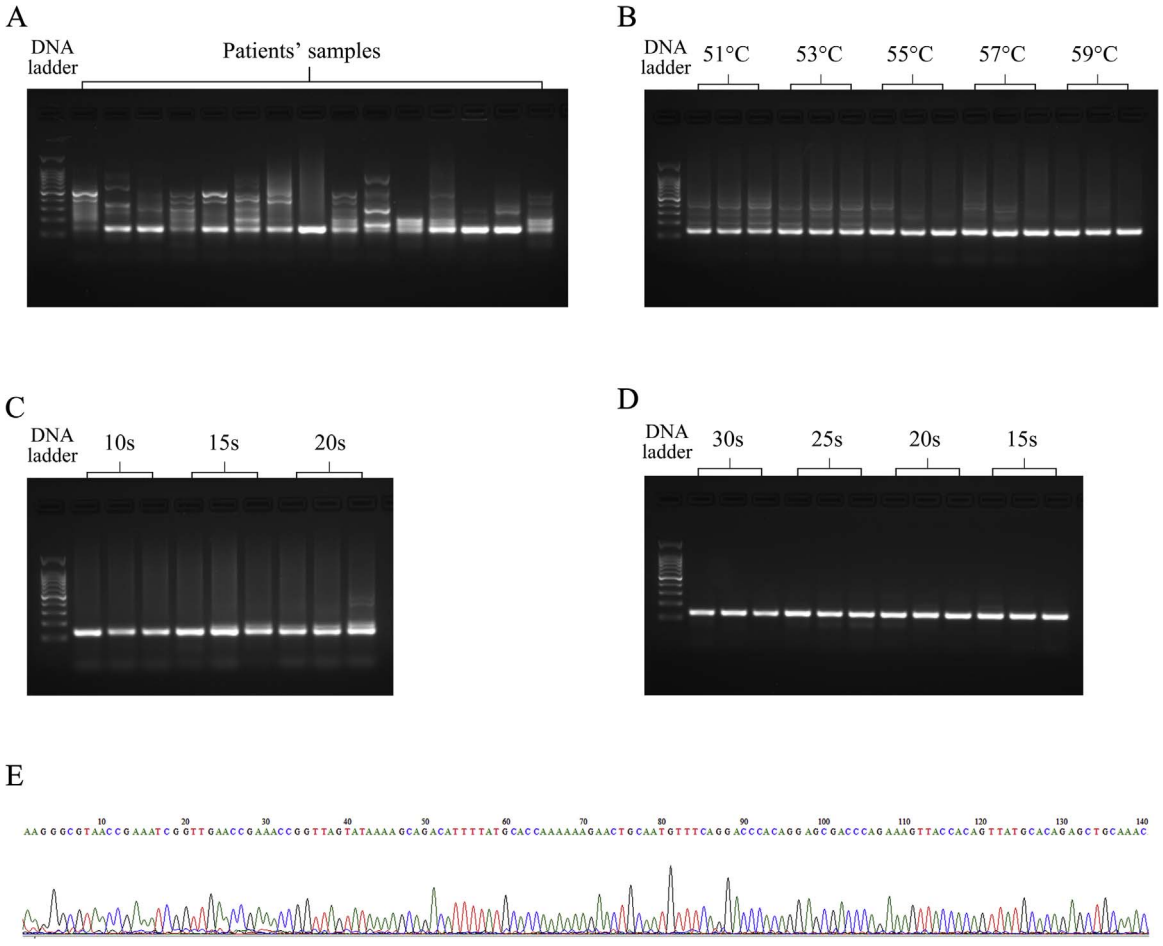

Fig. 4. The optimization of IR-COCONUT PCR parameters. (A) The gel electrophoresis results of different patient samples (lane 2 – lane 16). The sample with brightest target band was selected for the following optimization (B) The primer annealing temperature optimization indicated 59 °C as the optimized condition. (C) The extension time optimization indicated 10 s as the optimized condition. (D) The denaturation and annealing time optimization indicated 20 s as the optimized condition. (E) The monoclonal sequencing results of PCR products indicate the successful target gene amplification.

would occur at the conjugate pad and targeted DNA (biotin end) will be captured by streptavidin at the test line. After the solution migrated to the control line, the excess anti-digoxigenin-AP conjugates were captured by the goat-anti-rabbit IgG which were immobilized on the control zone. Then the BCIP/NBT stock solution was added to the sample pad. This solution was used as a substrate for the enzyme alkaline phosphatase. After the BCIP/NBT stock solution migrated to the test and control line, it would react both with the anti-digoxigenin-AP conjugates captured on the test zone and anti-digoxigenin-AP conjugates captured on the control zone and then formed visualizable purple sediments on these two sites. On the contrary, if the patient's cervical swab specimen was HPV 16 negative, the biotinylated forward primer would be captured by streptavidin at the test zone and anti-digoxigenin-AP conjugates would be captured by the goat-anti-rabbit IgG at the control zone. As a result, the BCIP/NBT stock solution would only react with anti-digoxigenin-AP conjugates captured on the control zone and formed only one visualizable purple sediments site.

3.4. Optimization and analytical performance of LFS

To reduce manual operation during detection process, a buffer chip (Supplementary Fig. 1) and LFS chip holder were plugged into the microfluidic PCR chip after amplification process through the inlet and outlet of the sample chamber (Fig. 5B). The buffer chip contains DI water and BCIP/NBT stock solution. Under the influence of gravity, PCR products, DI water and BCIP/NBT stock solution will flow onto the sample pad in sequence.

The intensity of test and control lines were greatly influenced by the loading amount of Anti-DIG-AP conjugates dispensed on the conjugate pad. The loading amount of the Anti-DIG-AP conjugates was varied from 50 ng to 100 ng (Fig. 5D, Supplementary Fig. 2) and 100 ng of Anti-DIG-AP conjugates was finally employed as the optimal amount.

At last, we examined the LFS performance in the presence of different concentration of target DNA (Supplementary Fig. 3). The intensity of the test line synchronized with the increase of DNA concentration which was proportional to 2^cycle number. Semi-quantitative detection of the target DNA was achieved by investigating the intensities of test line compared to control line from the resulting calibration curve (Fig. 5C & E).

4. Conclusions

We have developed a novel PCR platform named IR-COCONUT PCR. This novel platform offers accurate and flexible control of temperature through the integration of PID algorithms to manipulate the duty cycle of the voltage signals of IR LED and a peristaltic pump. The ramping rate of the introduced platform in current study is 1.5 °C/s for heating speed and −2.0 °C/s for cooling speed. This platform fulfills 30 thermal cycles within 50 min which is a match to the conventional bench-top PCR thermo cyclers. The PCR products were verified by LFS developed to be compatible with the PCR platform within 25 min. This PCR platform shows great potential for in-field and PoN testing of genetic or contagious diseases. Further work will aim to combine sample pretreatment onto the chip, reduce the overall thermal

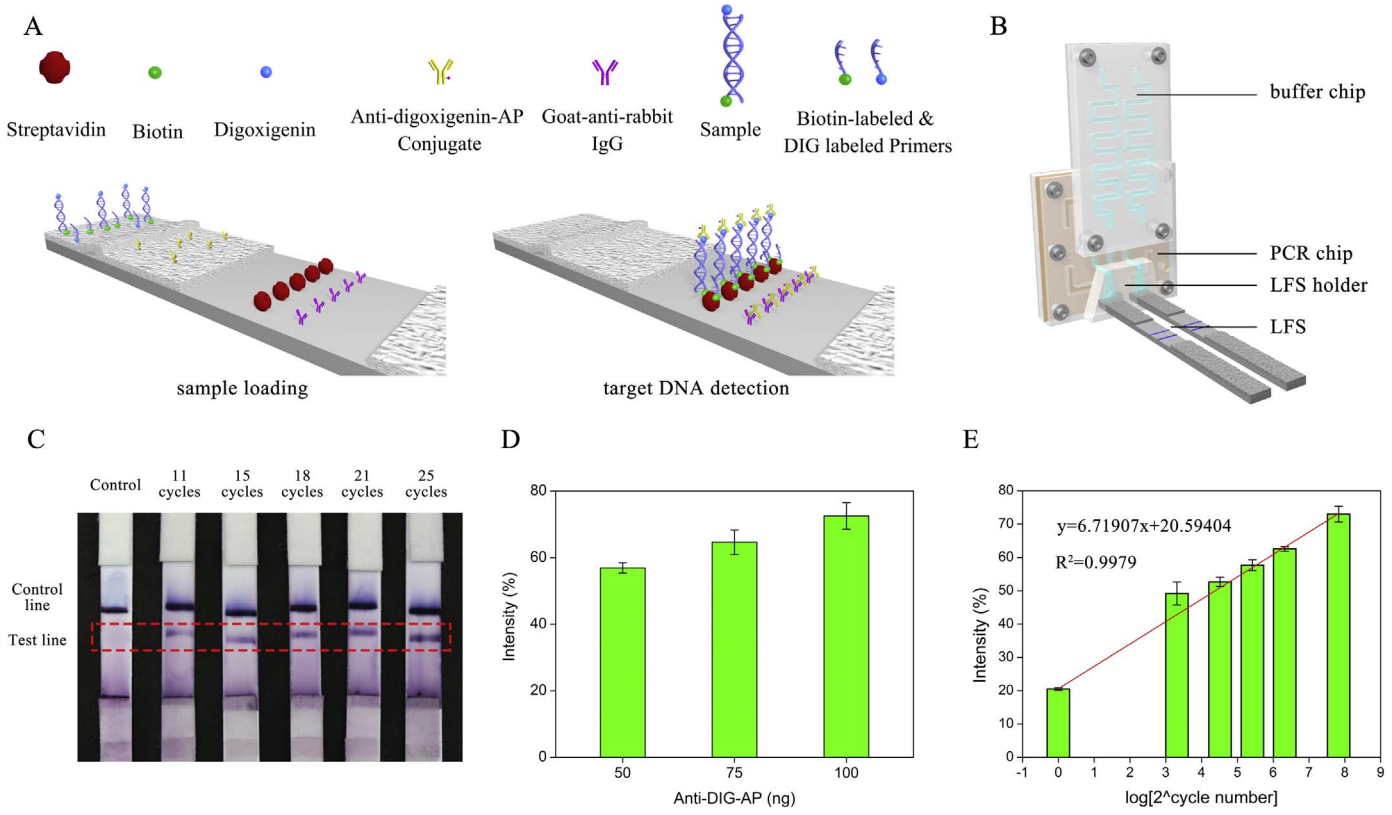

Fig. 5. Scheme of lateral flow strips (LFS) compatible with the presented platform for PCR product detection. (A) Illustration of the principle of HPV type 16 DNA measurement on LFS. (B) Schematic illustration of the assembly of buffer chip, PCR chip, LFS holder and LFS. (C) Typical image of LFS detection in the presence of different DNA concentrations. (D) The effect of Anti-DIG-AP concentration on color intensity of test line compared to control line. (E) The resulting calibration curve of different DNA concentrations. Bar plots represent Mean ± S.D. from 3 independent detections. (For interpretation of the references to color in this figure legend, the reader is referred to the web version of this article.)

mass by shrinking the volume of PCR chamber and utilizing in-situ fluorescence detection. Compared to the conventional lab equipment, the size of the present device is only 13 cm×15 cm×8 cm, with a weight of 460 g. Therefore, the present setup offers a solution for accurate and portable point-of-care PCR device.

Conflict of interest

The authors declare no conflict of interest.

Acknowledgements

This work was supported by National Natural Science Foundation of China (81301293) and China Major New Drugs Development Program (2014ZX09507008).

Appendix A. Supplementary material

Supplementary data associated with this article can be found in the online version at doi:10.1016/j.bios.2017.04.047.

References

Ahrberg, C.D., Ilic, B.R., Manz, A., Neužil, P., 2016. Handheld real-time PCR device. Lab a Chip 16 (3), 586–592.

Benjamin, R., Sébastien, C., 2016. Point-of-Need Testing: Application of Microfluidic Technologies. ⟨http://www.i-micronews.com/category-listing/product/point-of-need-testing-application-of-icrofluidic-technologies-2016-report.html?Utm_source=PR & utm_medium=email & utm_campaign=PoN_MarketOverview_Report_Oct2016⟩.

Bidmanova, S., Kotlanova, M., Rataj, T., Damborsky, J., Trtilek, M., Prokop, Z., 2016. Fluorescence-based biosensor for monitoring of environmental pollutants: from concept to field application. Biosens. Bioelectron. 84, 97–105.

Choi, J.R., Hu, J., Tang, R., Gong, Y., Feng, S., Ren, H., Wen, T., Li, X., Abas, W.A.B.W., Pingguan-Murphy, B., 2016. An integrated paper-based sample-to-answer biosensor for nucleic acid testing at the point of care. Lab a Chip 16 (3), 611–621.

Chuang, C.-H., Du, Y.-C., Wu, T.-F., Chen, C.-H., Lee, D.-H., Chen, S.-M., Huang, T.-C., Wu, H.-P., Shaikh, M.O., 2016. Immunosensor for the ultrasensitive and quantitative detection of bladder cancer in point of care testing. Biosens. Bioelectron. 84, 126–132.

Chung, K.H., Park, S.H., Choi, Y.H., 2010. A palmtop PCR system with a disposable polymer chip operated by the thermosiphon effect. Lab a Chip 10 (2), 202–210.

Gomes, H.I., Sales, M.G.F., 2015. Development of paper-based color test-strip for drug detection in aquatic environment: application to oxytetracycline. Biosens. Bioelectron. 65, 54–61.

Hühmer, A., Landers, J., 2000. Noncontact infrared-mediated thermocycling for effective polymerase chain reaction amplification of DNA in nanoliter volumes. Anal. Chem. 72 (21), 5507–5512.

Hagan, K.A., Reedy, C.R., Bienvenue, J.M., Dewald, A.H., Landers, J.P., 2011. A valveless microfluidic device for integrated solid phase extraction and polymerase chain reaction for short tandem repeat (STR) analysis. Analyst 136 (9), 1928–1937.

Lee, J.-H., Seo, H.S., Kwon, J.-H., Kim, H.-T., Kwon, K.C., Sim, S.J., Cha, Y.J., Lee, J., 2015. Multiplex diagnosis of viral infectious diseases (AIDS, hepatitis C, and hepatitis A) based on point of care lateral flow assay using engineered proteinticles. Biosens. Bioelectron. 69, 213–225.

Legendre, L.A., Bienvenue, J.M., Roper, M.G., Ferrance, J.P., Landers, J.P., 2006. A simple, valveless microfluidic sample preparation device for extraction and amplification of DNA from nanoliter-volume samples. Anal. Chem. 78 (5), 1444–1451.

Liu, R.H., Yang, J., Lenigk, R., Bonanno, J., Grodzinski, P., 2004. Self-contained, fully integrated biochip for sample preparation, polymerase chain reaction amplification, and DNA microarray detection. Anal. Chem. 76 (7), 1824–1831.

Neuzil, P., Zhang, C., Pipper, J., Oh, S., Zhuo, L., 2006. Ultra fast miniaturized real-time PCR: 40 cycles in less than six minutes. Nucleic Acids Res. 34 (11), e77, (e77).

Park, B.H., Oh, S.J., Jung, J.H., Choi, G., Seo, J.H., Lee, E.Y., Seo, T.S., 2016. An integrated rotary microfluidic system with DNA extraction, loop-mediated isothermal amplification, and lateral flow strip based detection for point-of-care pathogen diagnostics. Biosens. Bioelectron..

Qiu, W., Xu, H., Takalkar, S., Gurung, A.S., Liu, B., Zheng, Y., Guo, Z., Baloda, M., Baryeh, K., Liu, G., 2015. Carbon nanotube-based lateral flow biosensor for sensitive and rapid detection of DNA sequence. Biosens. Bioelectron. 64, 367–372.

Raeisossadati, M.J., Danesh, N.M., Borna, F., Gholamzad, M., Ramezani, M., Abnous, K., Taghdisi, S.M., 2016. Lateral flow based immunobiosensors for detection of food contaminants. Biosens. Bioelectron. 86, 235–246.

Raston, N.H.A., Nguyen, V.-T., Gu, M.B., 2016. A new lateral flow strip assay (LFSA) using a pair of aptamers for the detection of vaspin. Biosens. Bioelectron..

Rodriguez, N.M., Wong, W.S., Liu, L., Dewar, R., Klapperich, C.M., 2016. A fully integrated paperfluidic molecular diagnostic chip for the extraction, amplification, and detection of nucleic acids from clinical samples. Lab a Chip 16 (4), 753–763.
Slyadnev, M.N., Tanaka, Y., Tokeshi, M., Kitamori, T., 2001. Photothermal temperature control of a chemical reaction on a microchip using an infrared diode laser. Anal. Chem. 73 (16), 4037–4044.
Soejima, M., Koda, Y., 2014. Evaluation of point-of-care testing of C-reactive protein in forensic autopsy cases. Forensic Sci. Int. 237, 27–29.
Sposito, A., Hoang, V., DeVoe, D., 2016. Rapid real-time PCR and high resolution melt analysis in a self-filling thermoplastic chip. Lab a Chip 16 (18), 3524–3531.
Tarasov, A., Gray, D.W., Tsai, M.-Y., Shields, N., Montrose, A., Creedon, N., Lovera, P., O'Riordan, A., Mooney, M.H., Vogel, E.M., 2016. A potentiometric biosensor for rapid on-site disease diagnostics. Biosens. Bioelectron. 79, 669–678.
Wang, P., Ge, L., Yan, M., Song, X., Ge, S., Yu, J., 2012. Paper-based three-dimensional electrochemical immunodevice based on multi-walled carbon nanotubes functionalized paper for sensitive point-of-care testing. Biosens. Bioelectron. 32 (1), 238–243.
Wang, X., Yang, C., Zhu, S., Yan, M., Ge, S., Yu, J., 2017. 3D origami electrochemical device for sensitive Pb 2+ testing based on DNA functionalized iron-porphyrinic metal-organic framework. Biosens. Bioelectron. 87, 108–115.
Zhu, L., Zhu, C., Deng, G., Zhang, L., Zhao, S., Lin, J., Li, L., Jiao, P., Liao, M., Liu, Y., 2014. Rapid identification of H5 avian influenza virus in chicken throat swab specimens using microfluidic real-time RT-PCR. Anal. Methods 6 (8), 2628–2632.